JOURNAL OF MATERIALS SCIENCE **34** (1999) 3779–3787

Amorphous chalcogenide $Se_{1-x-y}Te_xP_y$ semiconducting alloys: thermal and mechanical properties

S. O. KASAP, T. WAGNER, V. AIYAH, O. KRYLOUK, A. BEKIROV
Electronic Materials Research Laboratories, Department of Electrical Engineering, University of Saskatchewan, Saskatoon, S7N 5A9, Canada
E-mail: kasap@engr.usask.ca

L. TICHY
Joint Laboratory of Solid State Chemistry of the Czech Academy of Sciences, Pardubice, Czech Republic

Thermal and mechanical properties of ternary Se rich $Se_{1-x-y}Te_xP_y$ semiconducting glasses (Te $<$ 20 at % and P $<$ 10 at %) in vitreous bulk and film form have been studied by differential scanning calorimetry (DSC) and microhardness measurements. Bulk vitreous samples were prepared by conventional melt quenching techniques and the amorphous photoreceptor films were prepared by vacuum deposition onto oxidized aluminum substrates whose electrophotographic properties were reported previously. We measured the glass transition temperature T_g starting from a well defined thermal history and using both heating and cooling scans as a function of composition. T_g increases monotonically with both Te and P content. Both bulk and film samples evince similar compositional T_g dependence. The increase in T_g with the P content in the glasses follows the Tanaka rule, that is, P addition has a networking effect due to the trivalent nature of the P atom and increases the mean coordination number. Both Te and P additions initially inhibit crystallization but at high Te contents (∼20 at %) the crystallization behavior is comparable to the pure a-Se case. Glasses with ∼10 at % Te seem to have the greatest resistance to crystallization. The crystallization behavior does not correlate with the T_g behavior over the whole composition range. The Vickers microhardness H_V increases with both Te and P content. H_V vs. Te and P behavior is similar to that of T_g vs. Te and P content . The compositional dependence of both H_V and T_g can be explained by the same factors that reduce Se chain mobility.

1. Introduction

Recently, there has been an increased interest in the properties of amorphous selenium (a-Se) rich semiconducting alloys due to their current uses as photoconductors in high definition TV pick-up tubes and, particularly, in digital X-ray imaging. Amorphous selenium binary alloys with tellurium, due to their electrophotographic applications such as photoreceptors in photocopying and laser printing, have been widely studied in both vacuum deposited amorphous film and vitreous bulk form in the past as reported and reviewed by a number of authors (see, for example, references [1–11] and references therein which cover a wide range of properties). Physical properties (e.g. density, hardness, glass transition temperature, electrical conductivity etc.) of binary vitreous Se:P alloys have been reviewed by Borisova [1] though experimental data for amorphous Se:P films is either very limited (e.g. [12]) or absent. Some of the most common physical properties of ternary Se:Te:P glasses such as the glass forming ability, density and electrical conductivity have been reported by a number of researchers as also summarized by Borisova [1]. Nearly all the measurements pertain to vitreous bulk samples quenched from the melt. There has been only one reported electrophotographic measurements on Se:Te:P vacuum deposited amorphous films which exhibit photosensitivity extending to the red region [13]. There have been no systematic studies on the thermal and mechanical properties of similar vacuum deposited a-Se:Te:P films which initiated the present study. Thermal and mechanical properties, such as the glass transition and crystallization temperatures and microhardness, are important factors in the potential use of these vitreous chalcogenide alloys in device applications [8, 9].

The physical properties of bulk glasses of the ternary Se:Te:P system or the binary Se:Te, Se:P systems have been usually reported either for very specific experimental conditions or without a full description of the experimental procedures. For example, the glass

transformation behavior of these alloys has been typically investigated by using differential thermal analysis (DTA) or differential scanning calorimetry (DSC) measurements under heating scans only. It is well known, however, that the glass transformation phenomenon as measured by heating scans exhibits dependence on the thermal history of each particular sample and, strictly, one cannot simply determine the effect of alloying on the glass transition temperature, T_g, without considering the thermal history of each particular sample of given composition. For example, it is generally found from DSC measurements that alloying of Se with Te increases T_g (e.g. [8, 9]) but in various other studies, such as in ultrasonic velocity vs. temperature [14] or volume vs. temperature measurements [15], T_g has been observed to decrease with the Te content. In this work we decided to examine the glass transition temperature by DSC under both heating and cooling scans. In carrying out DSC cooling scans, the vitreous specimen is heated to a temperature above its T_g at that heating rate. At this temperature, the structure is in the super- cooled liquid state or in liquid-like equilibrium state. The cooling scan at a constant cooling rate is then initiated from this temperature until the specimen becomes "glass". The glass transition temperature determined by this cooling DSC method does not show a dependence on the initial condition or the thermal history because in each case the sample starts from a liquid-like equilibrium state [16] (pure a-Se case was studied in reference [17]). In this work we carried out DSC experiments under both cooling and heating scans to obtain the thermal properties of both vitreous bulk samples and vacuum deposited amorphous photoreceptor films from the same bulk samples.

2. Experimental

2.1. Preparation of bulk glasses

$Se_{1-x-y}Te_xP_y$ alloys are glass formers [1]. Glassy $Se_{1-x-y}Te_xP_y$ alloy source material was prepared at the Joint Laboratory of Solid State Chemistry of the Czech Academy of Sciences and the University of Pardubice, Czech Republic, by combining a xerographic-grade fixed-composition amorphous Se:Te alloy with xerographic grade pure Se and phosphorus (red phosphorus from Fluka). Weighed amounts of Se:Te alloy, selenium and phosphorus were placed in a pre-cleaned and outgased quartz ampoule (by heating under vacuum to 900 °C) which was immediately evacuated to a pressure of 7.5×10^{-6} Torr for 30 min. The ampoule was then sealed, placed in a rotary furnace and heated to 600 °C for about 5–6 h. Following heating, the ampoule was cooled to 300 °C in the furnace and then it was taken out from the furnace and allowed to cool to room temperature. To prevent oxygen contamination, the alloys were kept sealed in the ampoule until they were needed for measurements as bulk samples or for the preparation of amorphous films.

2.2. Amorphous film deposition

Amorphous films of thickness 60–80 μm (typical photoreceptor film thicknesses) were prepared at the University of Saskatchewan (Electrical Engineering Materials and Devices Laboratories) by thermal evaporation of the $Se_{100-x-y}Te_xP_y$ alloy source material onto clean pre-oxidized aluminum substrates in a conventional vacuum coating system. Prior to the evaporation, the Al sheet substrate was degreased in trichloroethylene and then etched in a weak solution of trisodium phosphate and soda ash for 40 s at a temperature of 60 °C. Caustic residue on the substrate from the latter process was removed by dipping the substrate into a concentrated nitric acid solution (67%) for 5 min at room temperature. Finally the substrate was rinsed several times with deionized water. An oxide layer was grown on the substrate by placing it in a hot furnace (about 150 °C) for several hours. Thermal evaporation of the source material was accomplished by heating the alloy in an open stainless steel boat to a temperature of 350–390 °C in a vacuum of 5×10^{-6} Torr. The substrate temperature during the deposition process was about 75 °C. A typical deposition time for a 60 μm thick photoreceptor film was 15–20 min.

2.3. Content analysis

The tellurium and phosphorus contents were obtained by using an Elan Inductively Coupled Plasma-Mass Spectrometer (ICP-MS) in the Department of Geology. The Cl content in Cl doped Se-Te-P films are in the ppm level Cl (typically 2–10 ppm). It was not possible to obtain an accurate Cl analysis at the ppm level. Further, at ppm levels, Cl addition does not affect the thermal and mechanical properties of the alloy which depend primarily on the Se-Te-P composition. Generally, chlorine is added to Se:Te alloys to improve the electrophotographic properties [9, 18] but has no observable effect on the thermal and mechanical properties at these ppm levels.

2.4. Thermal properties

The thermal properties of bulk and film specimens were studied by differential scanning calorimetry (DSC). The bulk samples were crushed to small pieces and the film samples were stripped of their substrates after which they were placed in small aluminum pans and then sealed. An empty pan was used for reference. The specimen weight was typically kept below 30 mg to avoid the effects of finite thermal diffusivity of the sample on the measured transition temperatures. The experiments were carried out using a Mettler TA3000 thermal analysis system which consisted of a thermal analyzer (TC10) and a low temperature liquid nitrogen cell (DSC30), the latter allowing both heating and cooling schedules to be investigated at any selected rate. In a typical cooling scan DSC experiment for the measurement of T_g, the sample was heated from ambient temperature, $T_a = 25$ °C, at a rate of 20 °C min^{-1} to a temperature T_o well above its glass transformation region for that heating rate, but below the crystallization onset temperature. The cell was then stabilized at this temperature for about two minutes and then the cooling scan was initiated at a rate of 5 °C min^{-1}. The cooling

continued until the specimen past its glass transition temperature and was in the glassy state. The glass transition temperature T_g during cooling is denoted as T_{gc}. After the cooling scan, the sample was left to anneal at room temperature for approximately one month and then it was subjected to a heating schedule consisting of heating from $T_a = 25\,^{\circ}C$ at a rate of $5\,^{\circ}C\ min^{-1}$ to $300\,^{\circ}C$. It is important to note that the value of the glass transition temperature, T_{gh}, under a heating scan was measured for a sample with known thermal history which was set by the last cooling scan at a rate $5\,^{\circ}C\ min^{-1}$ and subsequent room temperature annealing. The DSC thermogram for a heating scan was also used to determine the crystallization onset temperature, T_{co}, maximum crystallization rate temperature, T_{cm}, melting temperature, T_m, and the enthalpy changes during these structural transformations. Heating and cooling DSC scans were carried out for both bulk and film samples to compare the compositional dependence of the glass transition temperature for both forms amorphous structure, bulk and film.

2.5. Mechanical properties

The microhardness measurements on amorphous Se:Te:P films were carried out in a standard way [19] using a 10 g load applied for a 10 s duration both of which were maintained the same for all the measurements. The Buehler Miromet II microhardness tester operates a diamond indenter for Vickers indentations on the test sample under the selected load for a selected duration. With a 10 g load, the measured indent diagonals were in the range 10–20 μm which corresponds to indentation depths much smaller than the film thicknesses. It is instructive to mention that Manika *et al.* [20] were able to show that microhardness measurements on amorphous films remain meaningful even when the indentation depth becomes comparable with the film thickness. The Vickers hardness number, H_V, was determined via the standard equation for H_V,

$$H_V = 1.854(F/d^2) \qquad (1)$$

where F is the load in kg and d the mean diagonal in μm.

3. Experimental results

Fig. 1 shows typical DSC thermograms observed in this work under a heating scan. All glass compositions studied exhibited a clear glass transition endotherm. However, only glasses with limited P content (a few atomic percent) evinced crystallization and melting peaks. The thermograms for Se-Te-P alloys with low P content (<1 at % P), in general, were similar to those reported previously for the Se:Te binary alloys [21]. Fig. 2 shows a typical DSC cooling scan where the glass transition is a change in the base line or a change in the heating capacity. Fig. 1 also identifies the experimental definitions used in this paper for the glass transformation onset temperature, T_{gh}, the crystallization onset temperature, T_{co}, the temperature for the maximum of the exothermic crystallization peak (or the temperature for maximum crystallization rate), T_{cm}, and the melting temperature, T_m. The glass transition temperature, T_{gc}, observed during cooling is operationally defined in Fig. 2. It should be emphasized that the glass transition temperature observed during cooling, T_{gc}, was independent of the initial temperature, T_o (provided that

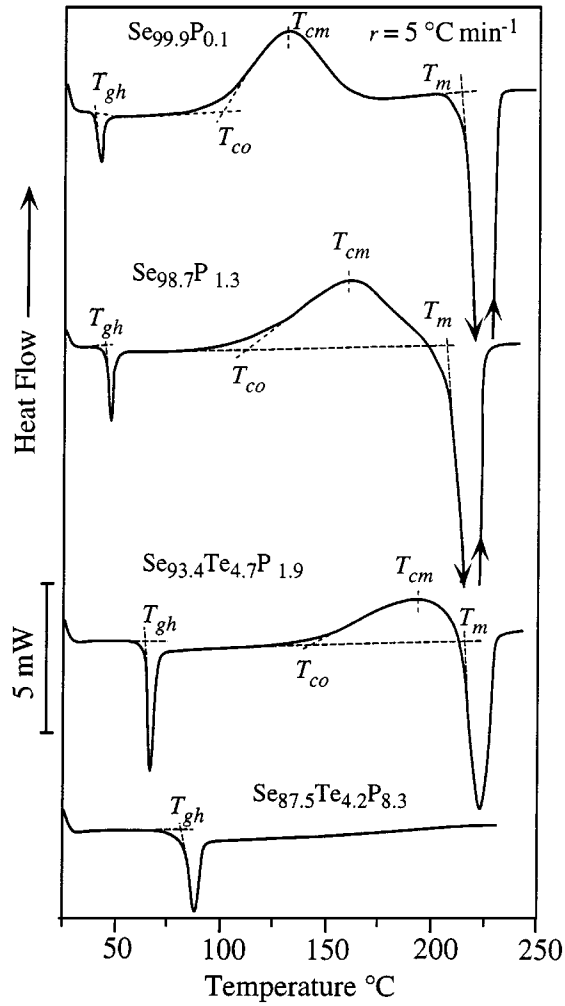

Figure 1 Typical DSC heating scan thermograms for Se-Te-P alloy film for compositions shown. All thermogramns are at the same heating rate of $5\,^{\circ}C\ min^{-1}$. Operational definitions for the glass transition temperature measured under a heating scan (T_{gh}), crystallization onset temperature (T_{co}), maximum crystallization rate temperature (T_{cm}) and the melting temperature (T_m) are also shown.

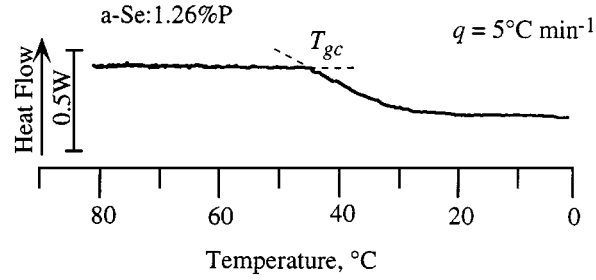

Figure 2 A typical DSC cooling scan for an a-Se:P film sample at a cooling rate of $5\,^{\circ}C\ min^{-1}$ after equilibration in the "liquid" region, above T_{gh} for heating. The operational definition of T_{gc} from a cooling is shown.

$T_o > T_{gh}$) and, furthermore, T_{gc}, as expected, was found to be independent of any thermal history. However, the glass transition temperature observed during heating, T_{gh}, was sensitive to the thermal history. Thus T_{gh} values from heating scans were obtained on samples annealed at room temperature as noted above.

All the experimental results are summarized in Tables I and II for vitreous bulk and amorphous film forms respectively. The plots described below were obtained from the data in these tables.

The three-dimensional plots of the compositional dependences of T_{gh} and T_{gc} for bulk and film $Se_{100-x-y}Te_xP_y$ alloys are shown in Figs 3a,b and 4a,b. It is apparent that the glass transition temperature increases with both Te and P contents. It can be seen that both bulk and film samples evince similar compositional T_g dependence.

Fig. 5a and b show the variation in the crystallization onset temperature as a function of Te and P content in bulk and film samples, respectively. The compositional dependence of the crystallization behavior does not follow the trend in the glass transition behavior in Figs 3 and 4. T_{co} exhibits a maximum as the Te concentration is increased in both bulk and film samples. On the other hand, T_{co} decreases with P alloying in bulk samples but remains relatively unaffected in film samples.

TABLE I Thermal properties of vitreous bulk samples

Se (at %)	Te (at %)	P (at %)	T_{gh} (°C)	T_{gc} (°C)	ΔH_{Tg} (J/g)	T_{co} (°C)	T_{cm} (°C)	ΔH_c (J/g)	T_m (°C)	ΔH_m (J/g)	T_g/T_m
100.0	0.0	0.0	44.0	41.6	3.3	129	147	59.7	215	68.4	0.644
99.9	0.0	0.1	44.2	41.5	1.8	113	185	26.5	218	39.2	0.641
99.8	0.0	0.2	46.1	42.3	2.0	104	183	21.9	215	62.2	0.646
98.9	0.0	1.1	47.9	45.5	3.3	111	173	15.1	213	17.5	0.655
98.7	0.0	1.3	51.0	48.0	4.0	118	182	7.9	214	14.3	0.659
91.4	0.0	8.6	77.3	75.5	4.3	165	175	1.7	188	4.6	0.756
90.6	0.0	9.4	76.4	79.5	4.2	116	170	2.0	180	6.5	0.778
99.94	0.06	0.0	47.6	41.7	3.6	136	158	63.4	216	72.2	0.643
99.7	0.3	0.0	48.0	42.0	3.4	127	146	62.0	218	73.9	0.641
99.4	0.6	0.0	48.1	42.5	3.5	141	164	63.4	218	73.3	0.641
98.8	1.2	0.0	48.3	42.8	3.5	131	151	60.9	218	73.3	0.643
96.5	3.5	0.0	50.6	43.7	3.9	132	145	58.6	223	72.2	0.639
93.6	6.4	0.0	53.8	47.1	4.3	144	156	56.5	227	70.1	0.640
90.2	9.8	0.0	57.3	49.1	4.8	149	160	55.8	232	73.2	0.637
80.6	19.6	0.0	62.4	56.5	4.4	125	137	47.7	245	79.2	0.636
90.8	7.2	2.0	61.5	55.8	5.7	141	174	3.8	213	5.9	0.675
88.3	9.7	2.0	63.6	55.4	5.5	140	192	6.6	218	6.0	0.670
88.0	7.0	5.0	73.1	67.5	6.1	131	180	1.6	203	1.1	0.715
85.6	9.4	5.0	82.3	85.2	5.9	—	—	—	—	—	—
83.4	6.6	10.0	82.6	82.1	6.3	—	—	—	—	—	—
81.1	8.9	10.0	87.3	92.4	4.5	—	—	—	—	—	—

Temperature parameters are defined in Figs 1 and 2.

TABLE II Thermal properties of vacuum coated amorphous films

Se (at %)	Te (at %)	P (at %)	T_{gh} (°C)	T_{gc} (°C)	ΔH_{Tg} (J/g)	T_{co} (°C)	T_{cm} (°C)	ΔH_c (J/g)	T_m (°C)	ΔH_m (J/g)	T_g/T_m	H_V (kgf/mm^2)
100.0	0.0	0.0	44.0	41.3	3.4	130	151	61.5	215	68.0	0.644	40.2
99.9	0.0	0.1	46.5	42.5	1.9	100	131	31.6	217	69.0	0.644	40.9
99.8	0.0	0.2	46.8	43.2	2.0	104	135	35.7	218	71.5	0.644	41.6
98.9	0.0	1.1	50.8	47.4	0.7	91	126	12.4	216	71.1	0.651	45.0
98.7	0.0	1.3	51.8	47.8	3.2	112	151	47.9	210	65.1	0.663	45.7
91.4	0.0	8.6	77.6	76.0	4.7	112	174	2.3	196	1.2	0.748	58.1
90.6	0.0	9.4	78.0	78.0	5.3	113	170	0.8	184	1.0	0.767	67.3
99.94	0.06	0.0	47.7	42.3	3.8	125	168	47.9	215	58.2	0.646	41.8
99.7	0.3	0.0	48.0	42.5	3.7	130	169	61.8	216	72.1	0.645	43.9
99.4	0.6	0.0	48.3	42.8	3.8	129	164	62.0	217	71.5	0.645	46.2
98.8	1.2	0.0	50.0	43.4	4.8	127	162	58.2	219	72.1	0.643	48.8
96.5	3.5	0.0	53.3	45.8	4.9	132	156	58.9	223	74.0	0.642	54.5
93.6	6.4	0.0	56.3	47.8	5.1	124	146	56.6	227	73.4	0.641	64.2
90.2	9.8	0.0	58.1	50.3	5.1	132	150	55.4	229	73.9	0.644	67.5
80.6	19.4	0.0	62.0	56.6	5.2	97	123	54.2	231	77.0	0.654	74.5
93.4	4.8	1.8	63.9	57.3	5.8	135	183	30.8	202	35.9	0.695	61.8
93.4	4.7	1.9	63.1	55.4	6.0	140	191	20.3	212	24.2	0.667	60.2
91.9	4.1	4.0	72.7	68.3	6.1	—	—	—	207	1.0	0.711	68.1
90.4	6.1	3.5	83.6	85.0	5.5	—	—	—	—	—	—	73.6
87.5	4.2	8.3	82.7	82.7	6.0	—	—	—	—	—	—	81.6
83.3	5.4	11.3	73.4	70.1	6.8	157	189	1.2	210	2.3	0.710	67.5

Temperature parameters are defined in Figs 1 and 2.

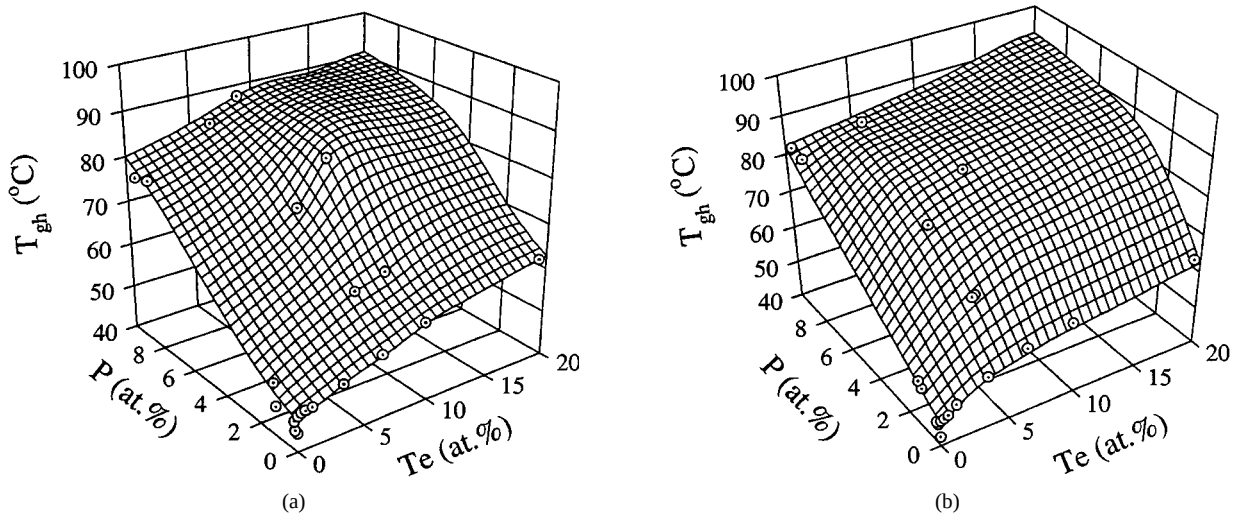

Figure 3 The dependence of T_{gh} (from heating scans) on the composition of amorphous Se-Te-P glasses: (a) bulk samples and (b) film samples.

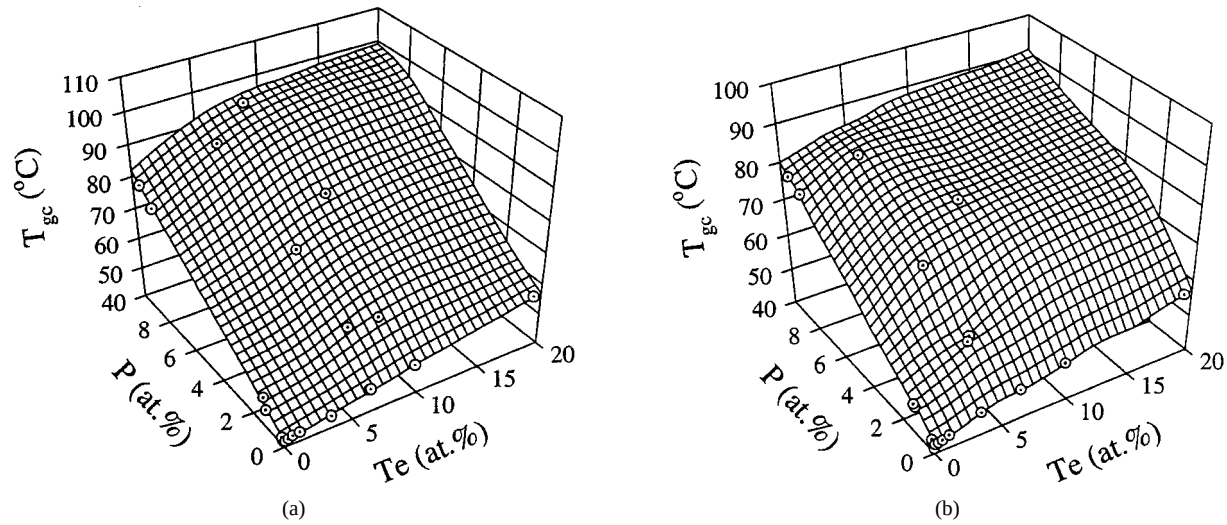

Figure 4 The dependence of T_{gc} (from cooling scans) on the composition of amorphous Se-Te-P glasses: (a) bulk samples and (b) film samples.

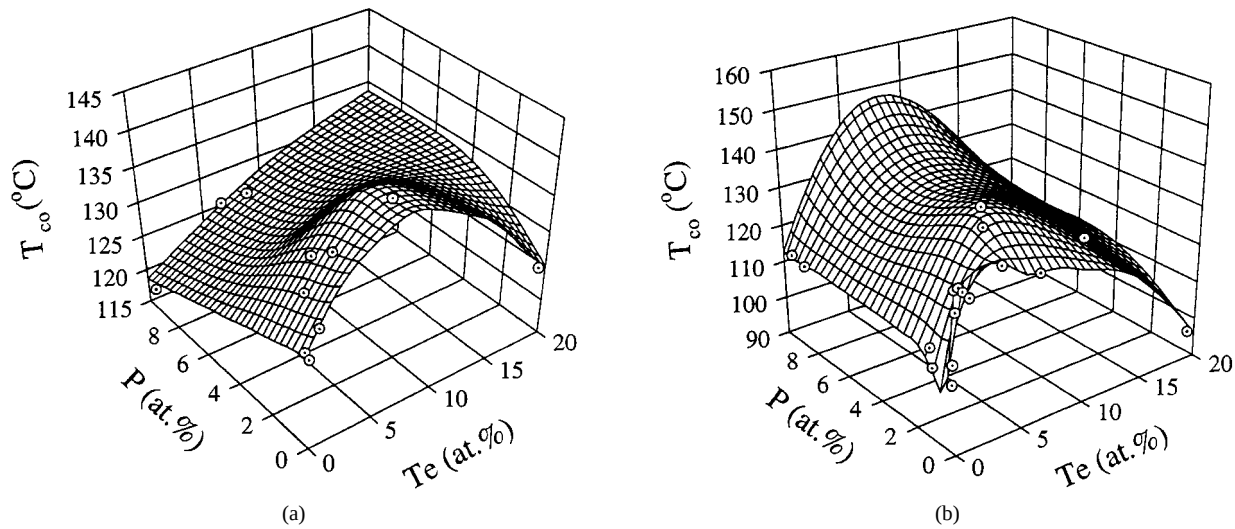

Figure 5 The dependence of the crystallization onset temperature T_{co} on the Se-Te-P glass composition for (a) bulk and (b) film samples.

The compositional dependence of the melting onset temperature, T_m, is presented in Fig. 6a and b for bulk and film samples respectively, where it can be seen that T_m decreases with P alloying but increases with Te alloying. However, T_m is difficult to discern clearly as the P concentration increases as apparent in Fig. 1.

Fig. 7a and b show the compositional dependence of the endothermic relaxation enthalpy ΔH_{Tg} associated

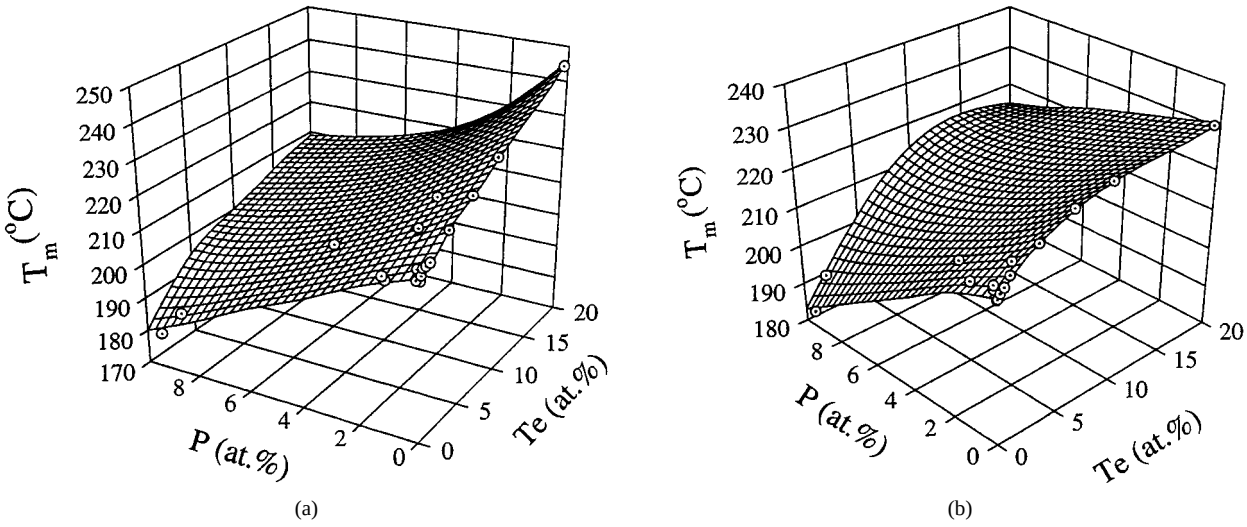

Figure 6 The dependence of the melting temperature T_m on the Se-Te-P glass composition for (a) bulk and (b) film samples.

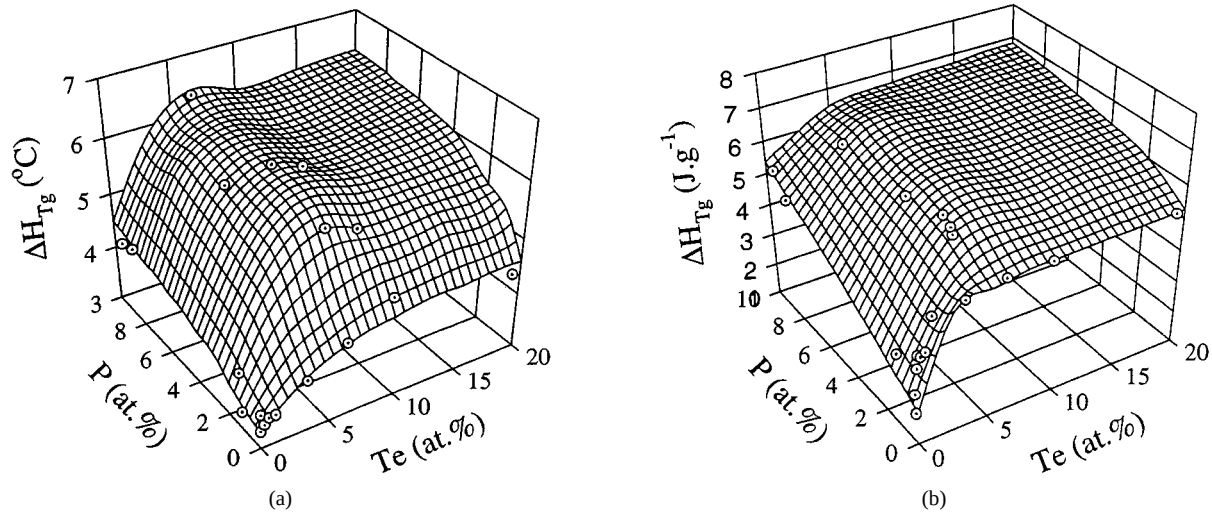

Figure 7 The dependence of the glass transition enthalpy ΔH_{Tg} (observed during heating scans) on the Se-Te-P glass composition for (a) bulk and (b) film samples.

with the glass transformation behavior during heating scans for bulk and film samples. The relaxation enthalpy increases with both Te and P contents. Many of the Se-Te-P ternary compositions did not exhibit a clearly discernible full crystallization exothermic peak that allows an unequivocal determination of the crystallization enthalpy; the crystallization process typically runs into melting as apparent for $Se_{98.7}P_{1.3}$, $Se_{93.4}Te_{4.7}P_{1.9}$ in Fig. 1. Further, as expected, those glasses that do not crystallize during heating also do not evince a clear melting endotherm. We were therefore unable to obtain accurate crystallization and melting enthalpies for these ternary alloys.

Microhardness of chalcogenide films is an important mechanical property in photoreceptor applications. We measured the Vickers microhardness for the $Se_{1-x-y}Te_xP_y$ film samples . All samples showed clear diamond Vickers indentations very similar to that reported for pure a-Se (see photograph in reference [22]). Fig. 8 shows the compositional dependence of H_V where it is apparent that the mechanical hardness increases monotonically with increasing Te and P contents. It should be noticed that the H_V vs. Te, P surface in Fig. 8 is very similar to that of the glass transition temperature, e.g. T_{gc} vs. Te, P surface in Fig. 4b.

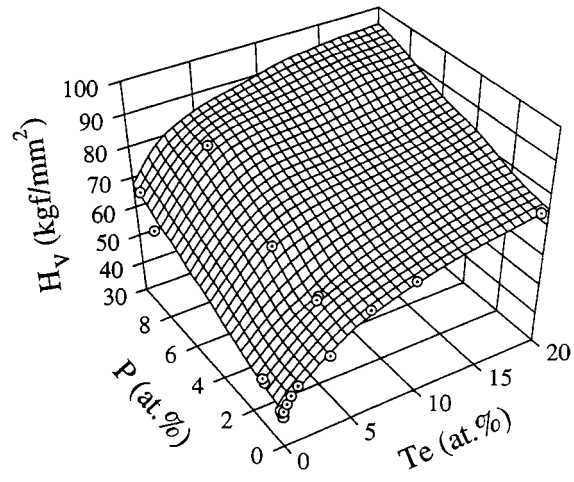

Figure 8 The dependence of Vickers microhardness on the Se-Te-P glass composition for film samples.

4. Discussion

We have observed that the glass transition temperature determined during cooling (T_{gc}) is independent of the initial cooling temperature but dependent on the cooling rate; the cooling rate dependence is not investigated in this work. However, the glass transition temperature observed during heating (T_{gh}) was sensitive to the thermal history which is an inherent feature of glasses; T_{gh} observed in heating scans depends on the thermal history as well as the heating rate. Both the thermal history and the heating rate were therefore kept the same for all the samples. The results show that T_{gc} and T_{gh} increase with Te and P concentrations and that both bulk and film forms of the amorphous state evince similar compositional T_g dependence. The T_{gc} and T_{gh} vs. P concentration behavior is steeper than that for the case of Te addition alone. The T_g values for the Se-P system, in general behavior, is in agreement with those for the same composition in references [1] and [12] where they have been determined by heating experiments rather than a controlled cooling scan. Compositional dependence of T_g can be explained qualitatively as follows.

Recent studies and experiments indicate that the structure of a-Se consists of randomly mixed long polymeric Se_n chains in which various portions of a chain have ring-fragments (e.g. [9, 23, 24]), in contrast to a structure which is a mixture of Se_n chains and Se_8 rings as thought in sixties and seventies. The average coordination number is two. Neutron diffraction study of $Se_{1-x}Te_{1-x}$ glasses ($x = 0$–40 at %) shows that tellurium short range order is mainly substitutional and average coordination number Z is kept almost constant; $Z \approx 2$ [25]. EXAFS (*extended X-ray absorption fine structure*) measurements [26] have validated above conclusions even in liquid $Se_{100-x}Te_x$ mixtures up to $x < 50$ at %. Although Te enters the structure by an isoelectronic substitution so that its coordination remains 2, there will nonetheless be changes in the van der Waals bonds, or interchain secondary bonds, because the Te atom is larger than the Se atom or put differently has more electrons in orbitals (both Se and Te have the same crystal structure, trigonal, which consists of chains that are held together by van der Waals bonds and the van der Waals interaction in Te crystals is stronger than that in Se crystals). One can therefore argue an increase in secondary bonding between chains as more Te added to the glass. Stronger secondary bonding and the increase in the average chain mass with Te addition lead to an increase in the glass transition temperature T_g. The addition of Te will also increase the concentration of charged valence alternation pair (VAP) type defects [8] so that it may argued that the increase in T_g is partly due to Se_3^+ and Te_3^+ type defects connecting neighboring chains and limiting molecular (chain) mobility. This argument is tantamount to the notion that the mean coordination number Z increases from 2 with Te addition. Mean coordination number in $Se_{1-x-y}Te_xP_y$ is defined by

$$Z = (1 - x - y)N_{Se} + xN_{Te} + yN_P \qquad (2)$$

where N_{Se}, N_{Te} and N_P are the normal coordination numbers of Se, Te and P ($N_{Se} = N_{Te} = 2$ and $N_P = 3$). However, the concentration of these VAP defects, due to the Boltzmann factor, is orders of magnitude smaller than the atomic concentration and it is unlikely that they will affect Z and hence the structure to an extent that T_g will be raised even though their influence on the electrical properties may be drastic [8, 9].

Phosphorus addition immediately increases the average coordination number from 2 since phosphorus, which is in Group V, can bond with 3 or 5 Se atoms. Three fold coordination will result in less structural strain than five fold coordination and would be more favorable. Phosphorus atoms in the structure can crosslink chains and hence enable a better covalent network structure to be developed. This leads to the observed steeper rise in T_g with P addition than in the case of Te addition alone as apparent in Fig. 3a and b and Fig. 4a and b. In the present range of P concentration (up to 10 at %), the concentration of phosphorus selenide like units (structural units $PSe_{3/2}$, $Se{=}PSe_{3/2}$ and $P_2Se_{4/2}$ where $=$ is a double bond) is expected to be so small that they do not form an independent framework. The glass structure in the present composition range is therefore primarily determined by the excess selenium and phosphorus atoms interlinking chains through covalent bonds [27].

The relationship between the observed T_g and the mean coordination number, according to Tanaka [28], can be empirically related by

$$\ln(T_g) = 1.6Z + C \qquad (3)$$

where Z is the mean coordination number ($1 < Z < 2.7$) as defined in Equation 2, and $C = 2.3$ Equation 3, of course, does not consider the rate of heating or cooling on T_g and therefore cannot be taken to be an exact relationship but rather a trend indicator. Typically, the relationship between $\ln(T_g)$ and the heating (r), or the cooling rate (q), is approximately also linear, i.e. $\ln(T_g) = Ar + B$ where A and B are constants. If we were to leave C as an adjustable parameter we can find C based on a-Se for which $Z = 2$. Taking $T_g = T_{gc} = 41.6 + 273$ K, gives $C = 2.55$. We can then examine Equation 3 for a-$Se_{90.7}P_{9.4}$ for which $T_{gc} = 79.5 + 273$ K. Equation 3 gives $Z = 2.071$. Assuming all P atoms are triply bonded (neglecting those in five-fold coordination and also the small fraction which also participate in VAP defect formation), we find the mean coordination number to be, $Z = (2 \times 0.907 + 3 \times 0.094) = 2.09$, close to the expected value. In the case of Se:Te:P glasses, of course, Equation 3 does not explain the rise in T_g with Te alloying as Te atoms do not increase the average coordination number. For example, both $Se_{81.1}Te_{8.9}P_{10}$ and $Se_{83.4}Te_{6.6}P_{10}$ glasses have approximately the same mean coordination, $Z = 2.1$, assuming that Te bonds with two neighbors but they have T_{gc} of 92.4 and 82.1 °C, respectively. It is, however, possible to explain the increase in T_g with Te addition by assuming that a small fraction of Te atoms are triply bonded so that they cross link chains. Then by using Equation 3 we can estimate the percentage of Te atoms in triple coordination. This turns out

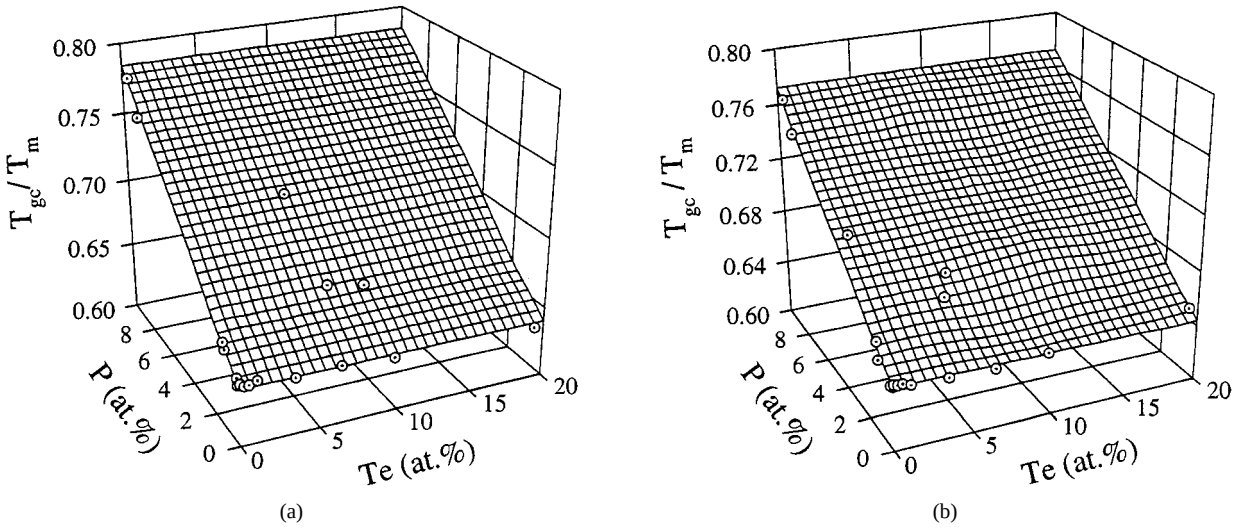

Figure 9 The dependence of T_{gc}/T_m on the Se-Te-P glass composition for (a) bulk and (b) film samples.

to be about 10–15% of all the Te atoms. There is no convincing justification for assuming that over ∼10% of the Te atoms in the structure are triply bonded given that neutron diffraction studies show no dramatic microstructural changes or other unusual features in the compositional range studied in this work [25].

It is well known that for many amorphous solids, glass transformation behavior as well as the rate of crystallization can be correlated with the viscosity, η. Indeed, experiments on pure a-Se show a good correlation between and the glass transformation and crystallization behavior and the viscosity [29]. The viscosity in $Se_{1-x}P_x$ binary glasses increases with the P content (up to 10 at%) [30, 31]. Although the increase in η with P content correlates well with the T_g behavior, there is no clear correlation with the onset of crystallization shown in Fig. 5. Furthermore, the viscosity of liquid Se-Te alloys, though in the liquid state, has been observed to decrease with increasing Te content [32] which certainly does not agree with the present observation of increase in T_g and also the initial increase in the crystallization temperature.

We have also examined the Kauzmann empirical rule $T_g/T_m \sim 2/3$, where T_m is the melting temperature, for the present glasses as shown in Fig. 9a and b for both bulk and film samples. We used T_{gc} (T_g from cooling scans) for the glass transition temperature and the standard operational definition of T_m in general thermal analysis (as in Fig. 1). Values of T_{gc}/T_m for Se:Te binary alloys are in the range 0.63–0.64 in close agreement with the Kauzmann rule given that T_{gc} also depends on the cooling rate. However, the ratio T_{gc}/T_m increases with the P content in the ternary alloys. At the highest P concentration this ratio is around ∼0.75 which is still not unusual given that for some network glasses T_g/T_m can be this high [33] and ratio itself depends on how T_g and T_m were actually measured. The melting temperature is progressively more difficult to discern as the P content increases. The crystallization exotherm becomes broader and melting begins before the whole sample has crystallized. One should use the liquidus temperature from the appropriate phase diagrams but these are not readily available for Se:Te:P ternary alloys. T_g/T_m values could only be evaluated for those samples which exhibited crystallization as summarized in Tables I and II.

In both Se:Te binary and Se:Te:P ternary alloys there is an initial increase in the crystallization temperature with Te alloying. The initial increase in the crystallization onset temperature correlates well with the increase in the glass transition temperature. The correlation is not unexpected as both would be controlled by the changes in the viscosity as the Te content is increased. Glasses with ∼10% Te have the greatest resistance to crystallization. At high Te concentrations there is a greater tendency to crystallize (crystallization onset temperature decreases with the Te content) which may be attributed to Te rich $Se_{1-x}Te_x$ glasses having a poor glass forming ability [34]. Glasses with considerable P content did not exhibit any crystallization exotherms as apparent in Fig. 1 but only a gradual melting process. This implies that trivalent P atoms in these chalcogen glasses, by virtue of their networking ability, are good glass formers [1].

Previous microhardness works have typically examined the microhardness of the binary glasses $Se_{1-y}P_y$ and $Se_{1-x}Te_x$ (e.g. [1, 9, 35]). The microhardness of both binary glasses has been reported to increase with the glass composition (P or Te) which is in agreement with the H_V vs. Te and H_V vs. P cuts on the surface in Fig. 8. The observed behavior of H_V in Fig. 8 correlates well with that of the glass transition temperature (both T_{gh} and T_{gc}) in Figs 3 and 4. One can argue that the same factors that increase T_g also increase H_V. Factors that limit relative chain flow (or increase the viscosity) would lead to a harder glass. The increase in H_V with Te addition is due to an increase in the strength of interchain secondary bonding whereas P addition leads to chain linking, or networking, by primary bonding.

5. Conclusions

Thermal and mechanical properties of ternary Se rich $Se_{1-x-y}Te_xP_y$ semiconducting glasses (Te < 20

at % and $P < 10$ at %) in bulk and vacuum deposited (photoreceptor type) film form have been studied by differential scanning calorimetry and microhardness measurements. We measured the glass transition temperature T_g starting from a well defined thermal history and using both heating and cooling scans as a function of composition.

The glass transition temperature T_g increases monotonically with both Te and P content. The increase in T_g with the P content in the glasses follows the Tanaka rule, that is, P addition has a networking effect due to the trivalent nature of the P atom and increases the mean coordination number. The increase in T_g with P content also correlates well with the reported increase in the viscosity with phosphor content in Se-P glasses. The increase in T_g with the Te addition is due to an increase in the interchain secondary bond strength and/or increase in the mean molecular (chain) mass since Te atoms maintain their two-fold coordination number in the structure. Both bulk and film samples evince similar compositional T_g dependence. Kauzmann ratio T_g/T_m for these ternary alloys was between 0.63 to 0.78.

Both Te and P additions initially inhibit crystallization. But at high Te contents ($\sim$20 at %) the crystallization behavior is comparable to the pure a-Se case. Glasses with $\sim$10 at %Te seem to have the greatest resistance to crystallization. The crystallization behavior does not correlate with the T_g behavior over the whole composition range.

The Vickers microhardness H_V increases with both Te and P content. H_V vs. Te and P behavior is *similar* to that of T_g vs. Te and P content . The compositional dependence of both H_V and T_g can be explained by the same factors that reduce Se chain mobility (or increase the viscosity).

Acknowledgements

Authors are grateful to Natural Sciences and Engineering Council of Canada and Noranda Advanced Materials (Quebec, Canada) for providing financial support for this project.

References

1. Z. U. BORISOVA, "Glassy Semiconductors" (Plenum Press, New Yok, 1981) pp. 215–220 and references therein.
2. M. F. KOTKATA and E. A. MAHMUD, *Mater. Sci. Eng.* **54** (1981) 168.
3. *Idem., ibid.* **54** (1982) 163.
4. M. ABKOWITZ and J. M. MARKOVICS, *Solid State Comm.* **44** (1982) 1431.
5. L. CHEUNG, G. M. T. FOLEY, P. FOURNIA and B. E. SPRINGETT, *Photog. Sci. Eng.* **26** (1982) 245.
6. M. ABKOWITZ and S. MAITRA, *J. Appl. Phys.* **61** (1987) 1038.
7. S. M. VAEZI-NEJAD and C. JUHASZ, *Sem. Sci. Technol.* **2** (1987) 809; **3** (1988) 664 and references therein.
8. B. E. SPRINGETT, *Phosphorus and Sulfur* **38** (1988) 341.
9. S. O. KASAP, "The Handbook of Imaging Materials" (Marcel Dekker, New York, 1991), Chap. 8, pp. 329–377 and references therein.
10. B. E. SPRINGETT, in "Proc. of the Fifth Int. Symp. on Uses of Selenium and Tellurium" (Selenium Tellurium Development Association, Brussels, Belgium, May 1994) pp. 187–190.
11. A. ONOZUKA, Y. NISHIKAWA and O. ODA, *Phosphorus and Sulfur* **38** (1988) 351.
12. R. BLACHNIK and A. HOPPE, *J. Non-Cryst. Solids* **34** (1979) 191.
13. S. O. KASAP, B. POLISHUK, V. AIYAH, A. BEKIROV, J. JAIN, A. BAILLIE, T. WAGNER and L. TICHY, *Can. J. Phys.* **70** (1992) 1118.
14. G. CARINI, M. CUTRONI, M. FEDERICO and G. GALLI, *J. Non-Cryst. Solids* **64** (1984) 317.
15. S. U. DZHALILOV and K. I. RZAEV, *Phys. Stat. Solidi.* **20** (1967) 261.
16. I. AVRAMOV and T. VASSILEV, *Poly. Ploy. Comp.* **2** (1994) 241 and references therein.
17. S. YANNACOPOULOS and S. O. KASAP *J. Mater. Res.* **5** (1990) 789.
18. Y. WANG and C. H. CHAMPNESS *J. Appl. Phys.* **77** (1995) 722.
19. ASTM, 1984, ASTM Standards Designation E384-73 entitled "Method for Microhardness of Materials," Vol. 02.05, pp. 653–657.
20. I. P. MANIKA, J. J. MANIKS and J. A. TETERIS, *J. Mater. Sci. Letts.* **7** (1987) 641.
21. S. O. KASAP and C. JUHASZ, *J. Mater. Sci.* **21** (1986) 1329.
22. S. O. KASAP, P. GUNDAPPA and S. YANNACOPOULOS, *J. Non-Cryst. Solids* **111** (1989) 82.
23. G. LUCOVSKY, in "The Physics of Selenium and Tellurium," Proc. of the International Conf. on the Physics of Selenium and Tellurium, Koigstein, Germany, edited by E. Gerlach and P. Grosse (Springer-Verlag, 1979) p. 178.
24. A. FELTZ, "Amorphous Inorganic Materials and Glasses" (VCH, Verlagsgesellschaft mbH, Weinhein, Germany, 1993, Chap. 3 and references therein.
25. R. BELLISENT and G. TOURAND, *J. Non-Cryst. Solids* **35**/**36** (1980) 1221.
26. K. TAMURA, M. INUI, M. YAO, H. ENDO, S. HOSOKAWA, H. HOSHINO, Y. KATAYAMA and K. MARUYAMA: *J. Phys.: Condens. Matter* **3** (1991) 7495.
27. D. LATHROP and H. ECKERT, *Phys. Rev. B* **43** (1991) 7279.
28. K. TANAKA, *Sol. State. Commun.* **54** (1985) 867–869.
29. S. O. KASAP and S. YANNACOPOULOS, *J. Mater. Res.* **4** (1989) 893.
30. E. I. KIM and G. M. ORLOVA, *Zh. Prikl. Khim.* **47** (1974) 989.
31. K. M. KHALILOV, B. B. KULIEV and F. A. GAMBAROV, *Phys. Stat. Solidi* **26** (1968) K113.
32. J. F. RIALLAND, J. C. PERON, in "Viscosity and Density of Se-Te Melts," Proc. 6th International Conference on Amorphous and Liquid Semiconductors 75' edited by B. T. Kolomiets (Iofee Fyz. Inst. Leningrad 1976) p. 371.
33. H. KANNO, *J. Non-Cryst. Solids* **44** (1981) 409.
34. M. T. MORA in "Amorphous Insulators and Semiconductors," edited by M. F. Thorpe and M. I. Mitkova (Kluwer Academic Publishers, Boston, MA, 1996) p. 45.
35. G. C. DAS, M. B. BEVER, D. R. UHLMANN and S. MOSS, *J. Non-Cryst. Solids* **7** (1972) 251–270.

Received 28 October 1997
and accepted 25 November 1998